

Photochromic Behavior of a Spiro-indolino-oxazine in Reverse-Mode Polymer-Dispersed Liquid Crystal Films

A. Romani,[†] G. Chidichimo,[‡] P. Formoso,[‡] S. Manfredi,[‡] G. Favaro,^{*,†} and U. Mazzucato[†]

Dipartimento di Chimica, Università di Perugia, 06123 Perugia, Italy, Dipartimento di Chimica, Università della Calabria, 87036 Rende (CS), Italy

Received: November 20, 2001; In Final Form: June 6, 2002

Based on the technology of polymer-dispersed liquid crystals (PDLC), this work deals with the preparation of bifunctional films sensitive to electric fields (changing transparency) and to light (changing color). Contrary to our recently proposed films working in the opaque \rightarrow transparent way on applying an electric field, the new films work in transparent \rightarrow opaque reverse mode. The spectroscopic and kinetic properties of a suitable photochromic compound of the spirooxazine series were preliminarily investigated in the separated constituents (monomer, polymerized monomer, and liquid crystal) of the PDLC matrix to evaluate the physical and chemical compatibility among components and the kinetic parameters of the color-forming and -bleaching processes. Thereafter, its behavior was studied in the reverse-mode PDLC films, which are naturally transparent in the absence of an electric field and become opaque on applying the field, while their color can be photochromically modulated by light exposure. The prototype of the photochromic reverse-mode film proposed in this work was found to be characterized by quite good electrooptical contrast, long-term stability, uniform droplet size distribution, and low driving fields.

Introduction

In the last years polymer-dispersed liquid crystal (PDLC)^{1–4} and emulsion-dispersed liquid crystal (EDLC)^{5,6} films have achieved great interest among electrooptical applications to build up large area panels for light transmission control. PDLC films are composite materials made by micron-sized droplets of low-molecular-weight liquid crystal embedded in a polymer matrix, while EDLC systems are constituted by homogeneous droplets of nematic material dispersed in continuous organic fluid matrix.

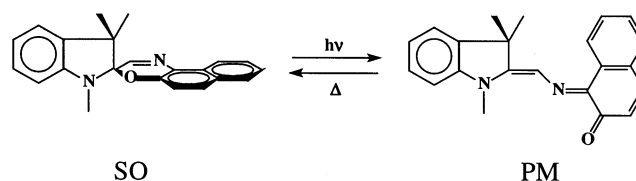
In both PDLC and EDLC films, the mismatching in the refractive indices of the matrix and the liquid crystal droplets causes a strong light scattering. In the normal mode operation, these films are naturally opaque (OFF state), while they become transparent (ON state) by application of a suitable electric field, which aligns the mesogenic molecules to match the ordinary liquid crystal refractive index to that of the polymer or monomer.

Recently, efforts have been devoted to obtain reverse-mode devices for applications requiring a naturally transparent OFF state electrically switchable into an opaque ON state. These electrooptical shutters are promising in view of a future involvement in the vehicles industry, building industry, and agriculture (greenhouses).

Inclusion of photochromic molecules in PDLC and EDLC matrixes was previously investigated to obtain bifunctional photochromic and electrooptical devices.^{7,8} The aim of this work was to prepare new bifunctional films working in the reverse-mode operation that could associate to the photochromic properties the possibility to modulate their transparency by means of electric fields.

Different methodologies have been proposed to prepare a reverse-mode system, such as the modification of the surface

SCHEME 1



energy of PDLC droplets,⁹ the use of dual-frequency addressable liquid crystals,^{10,11} the polymerization of nematic emulsions,¹² the use of mesogenic networks with a larger liquid crystal loading,^{13–15} and the use of the alignment properties of rough surfaces.^{16,17}

Our working strategy was to obtain bifunctional reverse-mode devices by adding photochromic compounds to the EDLC basic formulations, prepared with an UV polymerizable aliphatic urethane diacrylate. This allowed us to obtain reverse-mode PDLC starting from EDLC. These reverse-mode PDLC films are naturally transparent in the absence of an electric field and become opaque on applying the field; at the same time, the color can be modulated by light exposure because of the change in spectral properties of the photochrome upon UV irradiation. A new absorption band appears in the visible region and thermally disappears in the dark. The photochromic reaction leads to formation of a colored photomerocyanine (PM) from the colorless spirooxazine (SO), due to cleavage of the C–O spiro bond, Scheme 1.

In this work, electrooptical and morphological properties of the bifunctional reverse-mode PDLC films were investigated. Spectroscopic and kinetic properties of 6'-piperidine-1,3,3-trimethylspiro[indoline-2,3'-[3H]naphtho[2,1-b][1,4]oxazine] (SO) were investigated in the reverse-mode PDLC matrix and in its separated constituents (monomer, polymerized monomer, and liquid crystal) to evaluate the physical and chemical compatibility among components and the kinetic parameters of the

* To whom correspondence should be addressed. Fax number: +39-075 585 5598. E-mail: favaro@phch.chm.unipg.it.

[†] Università di Perugia.

[‡] Università della Calabria.

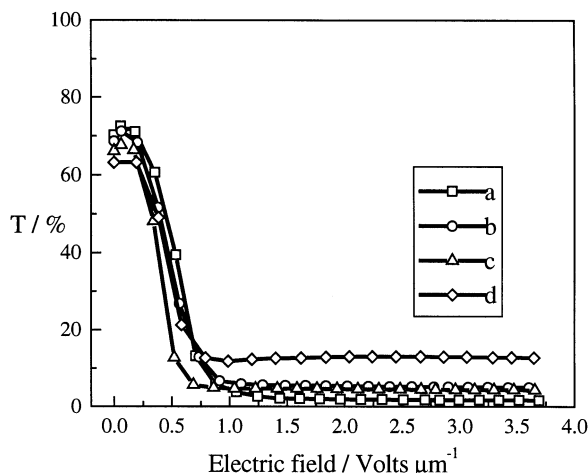


Figure 1. Electrooptical response of photochromic reverse-mode PDLC films containing (a) 0% SO, (b) 0.2% SO, (c) 0.33% SO, and (d) 0.5% SO.

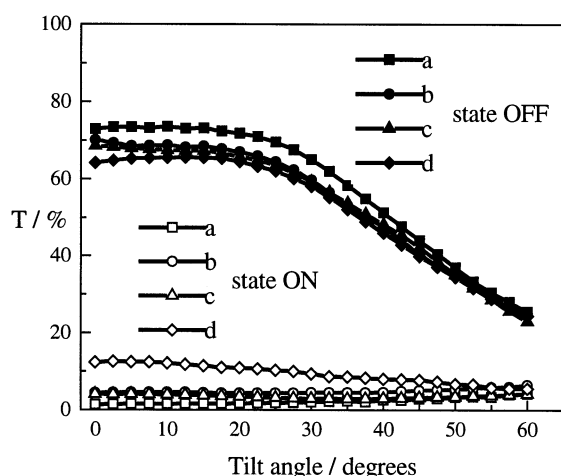


Figure 2. OFF and ON state transmittance dependence on the tilt angle of photochromic reverse-mode PDLC films containing (a) 0% SO, (b) 0.2% SO, (c) 0.33% SO, and (d) 0.5% SO.

confirmed by the angular OFF state transmittance reported in Figure 2, in which all samples show a monotonic transmittance decreasing as a function of the viewing angle.

We believe that the main role in the contrast ratio is played by the film morphology (droplet volume, density, and size), influenced by the different percentages of photochrome, rather than by the refractive index matching.^{3,4} Significant portions of droplet-free film volume were observed by optical microscopy. SEM analysis confirmed that, by increasing the quantity of SO (0.2% to 0.5%) dissolved in the films, a smaller number of droplets, characterized by a greater average size (3 to ~ 8 μm), separates. As a consequence of the increase in the droplet diameter, the field required for 90° orientation of the liquid crystal droplets decreases,^{3,4} as shown in Figure 1. Independent of the SO percentage, all films showed a higher uniformity and homogeneity in the droplet size distribution, as deduced from the electrooptical curves (Figure 1), which are sharper and shifted at lower voltage compared with those typical of conventional reverse-mode PDLC films.^{6,16,17}

Actually it is more difficult to make previsions about the influence that different amounts of SO can have on the equilibrium radius of the droplet. We can hypothesize that the photochrome affects more the surface tension at the interface than the liquid crystal elastic energy,⁸ thus reducing the

TABLE 1: Kinetic and Spectrophotometric Parameters for the Color-Forming and Thermal-Bleaching Processes of SO in LC Solutions at 293 K

% SO	α , s^{-1}	A_{PM}^∞	k_Δ , s^{-1}
0.2	0.26	0.21	0.27
0.33	0.31	0.17	0.25
0.5	0.30	0.20	0.25

anchoring strengths. However, more experimental data are needed to clarify this aspect.

Photokinetic Measurements. Measurements were first performed in the separated constituents of the PDLC to evaluate the physical, chemical, and photochemical compatibility of the photochrome with the matrix. For the purpose of comparison, some measurements were also carried out in two organic solvents of different viscosity and similar polarity.

The color-forming and color-bleaching kinetics were formally described by the monoexponential functions of eqs 1 and 2, respectively.

$$A_{\text{PM}} = A_{\text{PM}}^\infty (1 - e^{-\alpha t}) \quad (1)$$

$$A_{\text{PM}} = A_{\text{PM}}^\infty e^{-k_\Delta t} \quad (2)$$

For all systems, the absorbance at the wavelength of the PM spectral maximum, measured at the photostationary state (A_{PM}^∞), the kinetic parameter for the color-forming process (α), and the kinetic constant for the thermal bleaching (k_Δ) were determined by nonlinear fit of the experimental data sets (absorbance/time) to eqs 1 and 2. When photobleaching is neglected,¹⁹ the α parameter contains experimental factors, such as the intensity of incident light, I^0 , and properties intrinsic to the system, such as the quantum yield of the color-forming reaction, Φ , the molar absorption coefficient of the reactant at the irradiation wavelength, ϵ_{SO} , and the kinetic constant for the thermal bleaching, k_Δ (eq 3). The photokinetic factor $F = [1 - \exp(-2.3A_{\text{total}})]/A_{\text{total}}$ was kept constant by irradiating at an isosbestic point between the colorless and the colored forms. A_{PM}^∞ , which can be considered as a measure of the colorability of the photochromic system under the same experimental conditions, is given by eq 4, where ϵ_{PM} is the molar absorption coefficient of the colored form at the analysis wavelength and c_0 is the total photochrome concentration.²³

$$\alpha = \Phi I^0 F \epsilon_{\text{SO}} + k_\Delta \quad (3)$$

$$A_{\text{PM}}^\infty = \epsilon_{\text{PM}} \Phi I^0 F \epsilon_{\text{SO}} c_0 / \alpha \quad (4)$$

In principle, both the formation quantum yield and molar absorption coefficient of the metastable PM form can be obtained from eqs 3 and 4, if the intensity of the absorbed monochromatic light is known and the difference between α and k_Δ (eq 3) is significantly greater than the experimental uncertainty.

Measurements in Liquid Crystal. Color-forming and -bleaching kinetics of SO were carried out in the LC, using a 1 mm path cell and irradiating with all light emitted by the source at $\lambda > 350$ nm at room temperature ($T = 20 \pm 1$ $^\circ\text{C}$). Experimental results (see eqs 1 and 2) obtained at different SO concentrations are reported in Table 1. In Figure 3, three consecutive photo-coloration/bleaching cycles for the 0.2% SO solution are shown; in the inset, the spectrum of the metastable colored compound ($\lambda_{\text{max}} = 576$ nm) recorded at the photostationary state is reported. The high value of the absorbance background ($A = 0.42$) in the kinetic curves is due to turbidity of the nematic solvent.

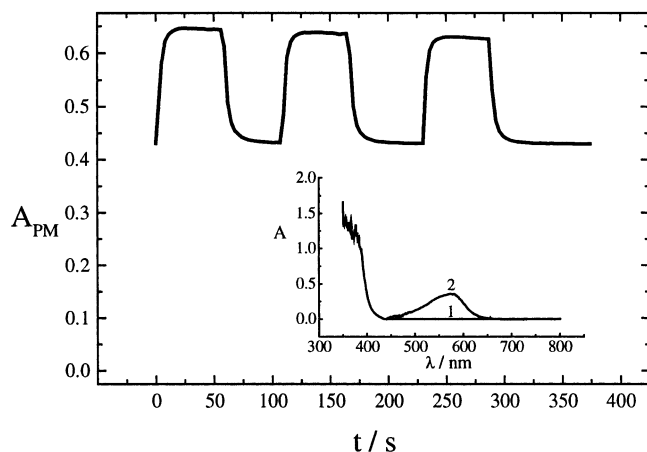


Figure 3. Consecutive color-forming and -bleaching processes of 0.2% SO in LC solution. The inset shows the absorption spectra in LC of the colorless SO (1) and the colored metastable PM recorded at the photostationary state (2).

The good reversibility of the system and the invariance of the kinetic parameters at different concentrations indicate an excellent compatibility of SO with the liquid crystal. Because α has approximately the same value as k_A , the color-forming rate is governed by the thermal back process, while colorability, A_{PM}^∞ , is practically insensitive to variation in the reactant concentration (see Table 1). This insensitivity can be attributed to fortuitous compensation due to decrease of F when the concentration increases. The k_A values are greater than those previously found in a liquid crystal (E49) used for direct-mode PDLC and EDLC.⁷ The increased rate of the process does not affect the color contrast, thus offering an additional interest of the system for potential applications.

Measurements in Monomer and Polymer. The photokinetic study of the photochromic system was carried out in the bulk components of the matrixes to be used for the bifunctional films, that is, the monomer (CN965) and polymerized monomer. In all of these media, the solubility requirements to obtain 0.2–0.5% SO solutions were fulfilled.

The color-forming kinetics was monitored at the maximum wavelength of the colored form, and the fit parameter, α (eq 1), was determined. The bleaching rates, k_A (eq 2), were easily obtained from the absorbance decay in the dark through monoexponential fit to first-order kinetics. Because of the different light paths of analysis (1 mm for the liquid crystal and about 30 μ m for the monomer and polymer measurements), the A_{PM}^∞ and α values obtained in polymer and monomer are not comparable with those in liquid crystal, while the k_A values can be compared for all measurements because temperature was kept constant. The bleaching rate decreases from liquid crystal to monomer and from monomer to polymer. The reversibility was fairly good as can be seen from Figure 4 in which consecutive coloration–decoloration cycles in both the monomer and polymer are shown. The results obtained for different SO concentrations in monomer and polymer films are shown in Table 2.

A structure change, such as that from a globular (SO) to a quasi-planar (PM) shape, and dipole moment changes occurring in the conversion $SO \xrightleftharpoons[h\nu]{\Delta} PM$ are responsible for the different dynamic responses to different environments. In Table 3, the wavelength maxima of PM, determined in all of the media investigated, are compared with those obtained in a polar (ethanol) and nonpolar (methylcyclohexane) solvent. The values

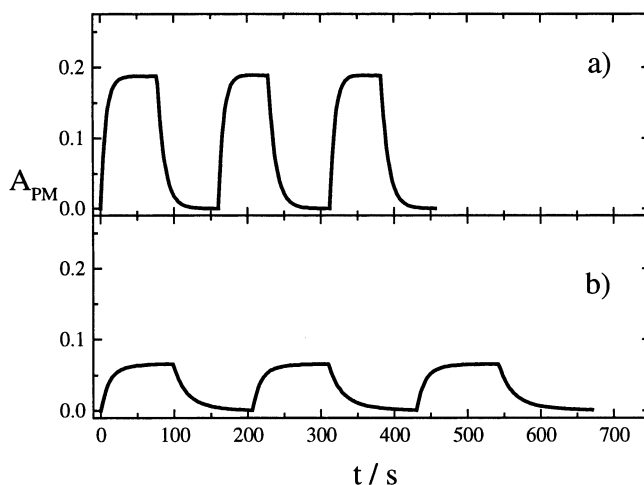


Figure 4. Consecutive color-forming and -bleaching processes of 0.5% SO in (a) monomer film and (b) polymer film.

TABLE 2: Kinetic and Spectrophotometric Parameters for the Color-Forming and Thermal-Bleaching Processes of SO in Monomer and Polymer Films at 293 K

composition	α , s ⁻¹	A_{PM}^∞	k_A , s ⁻¹
Monomer			
99.8% CN965 + 0.2% SO	0.138	0.185	0.100
99.67% CN965 + 0.33% SO	0.139	0.250	0.102
99.5% CN965 + 0.5% SO	0.140	0.190	0.103
Polymer			
98.8% CN965 + 0.2% SO + 1% IRGA	0.085	0.013	0.049
98.67% CN965 + 0.33% SO + 1% IRGA	0.081	0.040	0.047
98.5% CN965 + 0.5% SO + 1% IRGA	0.081	0.065	0.049

TABLE 3: Maximum Wavelength of the PM Metastable Colored Form in Different Media

medium	λ_{max}^{PM} , nm
methylcyclohexane ^a	550
ZLI 4788-000	576
PDLC	578
CN965 polymer	579
CN965 monomer	580
ethanol ^a	589

^a Values taken from ref 19.

indicate a similar polarity for all of the media investigated here, at an intermediate value between ethanol and methylcyclohexane. The wavelength change from LC (576 nm) to the monomer (580 nm) indicates a slight increase in polarity of the latter. Because of the relevant positive solvatochromism exhibited by SO in organic solvents,¹⁸ the ground state of PM is mainly represented by a quinoid nonpolar form, while its excited state is polar. Because the transition state for the ring-closure reaction was demonstrated to be very similar in polarity to the singlet excited state,¹⁸ an increase of medium polarity should favor the transition state and therefore fasten the thermal ring closure. The k_A values reported in the tables show that the thermal bleaching rate in the monomer is one-half of the value in liquid crystal. Going from monomer to polymer films, a further decrease of k_A was found, as evidenced in Figure 4. Normally, as the thermal bleaching rate increases, the colorability of a photochrome, that is, A_{PM}^∞ , is expected to decrease. This was not the case here, probably because of different filter-effects of the matrix on the light absorbed by the photochrome, which may affect the α value. The decreasing trend of the bleaching rate constant from liquid crystal to monomer and to polymer can be mainly ascribed to the increased viscosity of the matrix,

TABLE 4: Kinetic Parameters for the Color-Forming and -Bleaching Processes of SO in Ethylene Glycol ([SO] = 6.4×10^{-6} mol dm $^{-3}$, λ_{exc} = 400 nm) and Methanol ([SO] = 1.6×10^{-5} mol dm $^{-3}$, λ_{exc} = 388 nm) at Different Temperatures and Activation Energy, E_a , and Frequency Factor, A , for the Bleaching Process

T , K	α , s $^{-1}$	k_{Δ} , s $^{-1}$	E_a , kJ mol $^{-1}$	A , s $^{-1}$
Ethylene Glycol, $\epsilon_{(20^\circ\text{C})} = 37.7$, $\eta_{(20^\circ\text{C})} = 19.9$ cP ^a				
277.5	0.12	0.11	75	1×10^{13}
275	0.086	0.083		
272.5	0.056	0.057		
270	0.044	0.043		
267.5	0.033	0.033 ₅		
Methanol, $\epsilon_{(20^\circ\text{C})} = 32.66$, $\eta_{(20^\circ\text{C})} = 0.55$ cP ^a				
275	0.40	0.41	74	5×10^{13}
272.5	0.28	0.30		
270	0.19	0.20		
267.5	0.15	0.15		
265	0.11 ₅	0.11 ₅		
262.5	0.089	0.088		

^a Physical constants taken from ref 24.

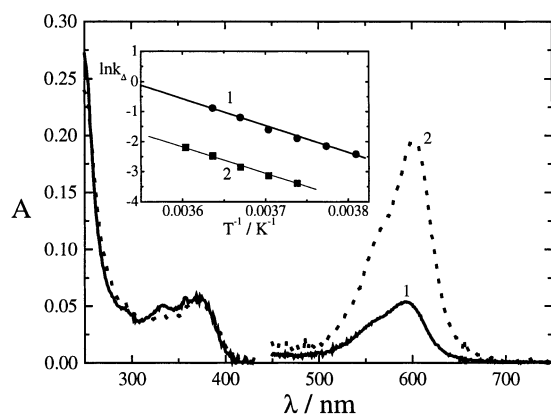


Figure 5. Spectra of the colorless SO form (250–410 nm) and of the irradiated solution at the photostationary state (450–700 nm) in methanol (1) and ethylene glycol (2) at 270 K and λ_{exc} = 370 nm. The inset shows Arrhenius plots for the bleaching kinetics.

which affects the rate of the geometric rearrangements that change the structure from planar (PM) to globular (SO).

Measurements in Organic Solvents. To support this hypothesis, kinetic measurements of the color-bleaching process were performed in methanol and ethylene glycol. These solvents have similar polarities ($\epsilon_{(20^\circ\text{C})} = 32.66$ and 37.7 , respectively) but very different viscosities ($\eta_{(20^\circ\text{C})} = 0.55$ and 19.9 cP, respectively).²⁴ Because of scant solubility of SO in ethylene glycol, the absorbance of the studied solutions ([SO] = 6.4×10^{-6} mol dm $^{-3}$) at the irradiation wavelength (λ_{exc} = 400 nm) was very small ($A_{\text{SO}} = 0.016$). Under these experimental conditions, the bleaching rate was too fast to obtain a reliably measurable absorbance of the colored form at room temperature. To increase the PM amount at the photostationary state, temperature was lowered. Kinetic parameters for the forward photoreaction and back thermal bleaching were determined in the 262–277 K temperature range to estimate the activation energy for the thermal process (Table 4). The spectra at 270 K of the closed form and at the photostationary state in both solvents are shown in Figure 5. In the inset, Arrhenius plots for the thermal bleaching show a parallel trend in the two solvents indicating a similar activation energy ($E_a = 75$ kJ mol $^{-1}$ in EtGly and 74 kJ mol $^{-1}$ in MeOH) and slightly different frequency factors (5×10^{13} and 1×10^{13} s $^{-1}$ in MeOH and EtGly, respectively). The latter is responsible for the difference in the bleaching constants. Looking at the wavelength maxima (602 nm in EtGly

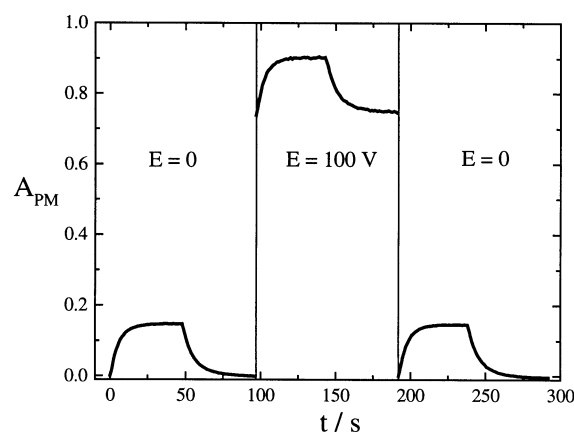


Figure 6. Consecutive color-forming and -bleaching processes of 0.33% SO in PDLC in the absence and in the presence of electric field at 293 K.

TABLE 5: Kinetic and Spectrophotometric Parameters for the Color-Forming and Thermal-Bleaching Processes of SO in PDLC (30 μ) in the Absence and in the Presence of Electric Field at 293 K

	$E = 0$ V/ μm			$E = 100$ V/ μm			$E = 0$ V/ μm		
% SO	α , s $^{-1}$	A^∞	k_{Δ} , s $^{-1}$	α , s $^{-1}$	A^∞	k_{Δ} , s $^{-1}$	α , s $^{-1}$	A^∞	k_{Δ} , s $^{-1}$
0.2	0.163	0.009	0.126	0.206	0.009	0.065	0.214	0.006	0.099
0.33	0.185	0.120	0.136	0.195	0.128	0.129	0.183	0.123	0.133
0.5	0.170	0.151	0.131	0.181	0.168	0.126	0.174	0.151	0.123

and 594 nm in MeOH), one can infer that the excited molecule exploits a more polar environment in the viscous solvent, which could cause an increase of rate of the ring-closure process,²² in contrast with observation. Thus, it can be concluded that the rate of the thermal process is dominated by viscosity. Consequently, colorability is greater in EtGly than in EtOH. To evaluate the quantum yield and molar absorption coefficient of the colored form, previously developed methods^{24,25} were tentatively applied. However, because of the low absorbance values, the determinations were very uncertain and only allowed the product $\Phi\epsilon$ to be determined. The $\Phi\epsilon$ values were very similar in the two solvents. By using the ϵ value previously obtained in ethanol ($67\,000$ dm 3 mol $^{-1}$ cm $^{-1}$), which is a reasonable approximation, $\Phi = 0.40$ and 0.44 were obtained in MeOH and EtGly, respectively. These quantum yield values are in line with those determined in EtOH (0.65) considering that the experimental uncertainty is about 15%.

Measurements in PDLC. Measurements on PDLC films containing SO were performed using the same SO concentrations as those in liquid crystal and in monomer and polymer films. Photokinetic and spectrophotometric parameters were determined for three consecutive coloration and decoloration cycles in the absence, in the presence, and again in the absence of electric field. In Figure 6, the kinetic trends for the 0.33% SO sample are shown. In the absence of electric field and in the dark, the film was transparent and colorless. It changed color under irradiation and bleached in the dark. When a 100 V driving voltage was applied, the system became markedly opaque (absorbance ≈ 1), whereas the coloration–decoloration cycles remained practically unchanged. After removing the electric field, the initial conditions were completely restored and the system reproduced the same photochromic behavior. Color-forming and -bleaching kinetics for all cycles fit to a monoexponential function well. The parameters obtained are resumed in Table 5. The concentration effect is seen in the α value, which decreases with increasing the SO concentration because of a decreased photokinetic factor, and in the A_{PM}^∞

TABLE 6: Effect of LC Percent on the Bleaching Parameter Determined in CN965 Polymeric Films Containing 0.33% SO at 293 K

LC %	k_A , s ⁻¹
0	0.047
2	0.062
5	0.068
7	0.071
10	0.083
20	0.095
30	0.099
40	0.11

value, which increases with the SO concentration. The data for the 0.2% SO sample are affected by larger errors due to the very low photoconversion percentage ($A_{PM}^\infty < 0.01$). Because the k_A values are significantly different in the polymer ($k_A = 0.048$ s⁻¹) and liquid crystal ($k_A = 0.25$ s⁻¹) separate phases, we would have expected a dual contribution to the color-forming and color-bleaching kinetics. In contrast, all kinetics that were tested on several PDLC samples were found to be monoexponential, yielding a kinetic parameter ($k_A = 0.11$ s⁻¹) intermediate between that in polymer and that in liquid crystal. This behavior suggests that the photochrome is preferentially located in a pseudohomogeneous phase having intermediate properties between those of the polymer and the liquid crystal.

To support this hypothesis, we performed coloration–decoloration experiments on CN965 polymeric films containing 0.33% SO and measured the k_A value at gradually increasing LC percentages. No phase separation was observed up to 10% concentration. Above this value, the system separates into two (liquid-crystal-rich and polymer-rich) phases. When the analytical content of the liquid crystal is increased, its concentration in the polymer matrix continues to increase to finally reach the saturation value, controlled by the partition equilibrium.

The k_A value (Table 6) measured in these films rapidly increases with the liquid crystal percentage, up to ~10% LC, and then, it slowly reaches the limit value of 0.11 s⁻¹. This result strongly suggests that the photochrome is confined into the polymeric phase, plasticized by the liquid crystal, because the increase of k_A with the liquid crystal analytical percentage follows a trend similar to that of the liquid crystal amount trapped into the nematic swollen-polymeric phase. In other words, we believe that the photochrome, being confined into the polymer-rich phase, bleaches at a gradually faster rate on increasing the liquid crystal concentration because of the plasticizer effect of the LC on the polymer film, which gradually reduces its viscosity. Even if this explanation for the monoexponential trend appears to be reasonable, further work is needed to better clarify this behavior.

Conclusions

This paper shows that bifunctional reverse-mode PDLC films, which are able to change transparency as a function of external electric fields and color under light irradiation, can be obtained by polymerization of photochromic nematic emulsions. The photochromic reverse-mode films proposed in this work are characterized by quite good electrooptical contrasts, long-term stability (no evidence of electrooptical change was observed

after 6 months from the time of sample preparation), uniform droplet size distribution (independent of the amount of SO dissolved), and low driving fields.

The results obtained from the photokinetic study of SO in reverse-mode PDLC films and in the constituents of this matrix indicate a remarkable effect of the medium viscosity on the color-forming and -bleaching kinetic parameters. This effect is assigned to entropic factors.

This bifunctional system is very promising for future applications because the photochrome stability appears good and colorability of the films is high enough in both the transparent medium (electric field OFF) and the opaque one (electric field ON). Compared with direct-mode PDLC,⁸ the photochemical process is cleaner and the system exhibits better colorability and reversibility.

Acknowledgment. This research work was carried out in the framework of the Progetto Finalizzato “Materiali Speciali per Tecnologie Avanzate II” of the Italian National Research Council. It was partially funded also by the Ministero per l’Università e la Ricerca Scientifica e Tecnologica (Rome) and the Perugia University in the framework of the “Programmi di Ricerca di Interesse Nazionale”.

References and Notes

- (1) Ferguson, J. L. U. S. Patent No. 4,435,047, 1984.
- (2) Doane, J. W.; Chidichimo, G.; Vaz, N. U. S. Patent No. 4,688,900, 1987.
- (3) Doane, J. W. In *Liquid Crystal: Applications and Uses*; Bahadur, B., Ed.; World Scientific: Singapore, 1990; Chapter XIV, p 361.
- (4) Drzaic, P. S. *Liquid Crystal Dispersions*; World Scientific: Singapore, 1995.
- (5) De Filpo, G.; Lanzo, G. J.; Nicoletta, F. P.; Chidichimo, G. *J. Appl. Phys.* **1998**, *84*, 3581.
- (6) De Filpo, G.; Lanzo, G. J.; Nicoletta, F. P.; Chidichimo, G. *J. Appl. Phys.* **1999**, *85*, 2894.
- (7) Favaro, G.; Chidichimo, G.; Formoso, P.; Manfredi, S.; Mazzucato, U.; Romani, A. *J. Photochem. Photobiol. A: Chem.* **2001**, *140*, 229.
- (8) Chidichimo, G.; Formoso, P.; Manfredi, S.; Favaro, G.; Mazzucato, U.; Romani, A. *J. Appl. Phys.* **2001**, *90*, 4906.
- (9) Ma, Y. D.; Wu, B. G.; Xu, G. *Proc. SPIE* **1990**, *46*, 1257.
- (10) Nolan, P.; Coates, D. *Mol. Cryst. Liq. Cryst. Lett.* **1991**, *8*, 75.
- (11) Gotoh, T.; Murai, H. *J. Appl. Phys.* **1992**, *60*, 392.
- (12) Nicoletta, F. P.; De Filpo, G.; Lanzo, J.; Chidichimo, G. *J. Appl. Phys. Lett.* **1999**, *74*, 3945.
- (13) Hikmet, R. A. M. *J. Appl. Phys.* **1990**, *68*, 1.
- (14) Hikmet, R. A. M.; Zwerver, B. H. *Liq. Cryst.* **1992**, *12*, 319.
- (15) Yang, D. K.; Chien, L. C.; Doane, J. W. *J. Appl. Phys. Lett.* **1992**, *60*, 3102.
- (16) Macchione, M.; Cupelli, D.; De Filpo, G.; Nicoletta, F. P.; Chidichimo, G. *Liq. Cryst.* **2000**, *27*, 917.
- (17) Macchione, M.; Cupelli, D.; De Filpo, G.; Nicoletta, F. P.; Chidichimo, G. *Liq. Cryst.* **2000**, *27*, 1337.
- (18) Favaro, G.; Masetti, F.; Mazzucato, U.; Ottavi, G.; Allegrini, P.; Malatesta, V. *J. Chem. Soc., Faraday Trans.* **1994**, *90*, 333.
- (19) Favaro, G.; Malatesta, V.; Mazzucato, U.; Ottavi, G.; Romani, A. *J. Photochem. Photobiol. A: Chem.* **1995**, *87*, 235.
- (20) Wilkinson, F.; Hobley, J.; Naftaly, M. *J. Chem. Soc., Faraday Trans.* **1992**, *88*, 1511.
- (21) Favaro, G.; Ortica, F.; Malatesta, V. *J. Chem. Soc., Faraday Trans.* **1995**, *91*, 4099.
- (22) Ortica, F.; Favaro, G. *J. Phys. Chem. B* **2000**, *104*, 12179.
- (23) Ottavi, G.; Ortica, F.; Favaro, G. *Int. J. Chem. Kinet.* **1999**, *31*, 303.
- (24) Scaiano, J. *Handbook of Organic Photochemistry*, Vol. II; CRC Press Inc: Boca Raton, FL, 1989; p 344.
- (25) Favaro, G.; Romani, A.; Becker, R. S. *Photochem. Photobiol.* **2000**, *72*, 632.